Iraqi J. Laser, Part A, Vol.12, pp. 15-25 (2013)

IRAQI JOURNAL OF LASER

Refractive Index Scaling in Hollow Core Photonic Crystal Fiber

Dalya H. Abbas and **Abd-Alhadi M. Al-Janabi**

Institute of laser for postgraduate studies, University of Baghdad, Iraq

(Received 24 April 2012; accepted 24 September 2013)

Abstract:In this paper, simulation study of the frequency shift of photonic bandgaps due to refractive index scaling using liquids filled hollow-core photonic crystal fibers is presented. Different liquids (distilled water, n-hexane, methanol, ethanol and acetone) are used to fill the cladding of 2 types of hollow core photonic crystal fibers (HC19-1060, HC7-1060). These liquids are used to change the effective index scaling and index contrast of the cladding. The effect of increasing temperature of the liquid (20-100 ^{0}C for water and 20-70 ^{0}C for other liquids) infiltrated hollow core fiber on the bandgap width and transmission properties has been computed. The maximum photonic bandgap width at 0.0243 has appeared with filling HC7-1060 PCF with methanol at 70 ^{0}C at a corresponding refractive index 1.3057. Photonic bandgap structure for both TE and TM modes of a 2D photonic crystal with triangular lattice of air holes embedded in silica background material was studied using Plane Wave Expansion (PWE) method to find the width of photonic bandgap finger in photonic crystal states diagram.

Introduction

In the past few years, photonic crystal fibers (PCFs) have attracted considerable interest as an alternative to conventional optical fibers in many applications [1]. PCFs are a class of single-material (typically silica). Optical fibers consist of a central defect region surrounded by a regular pattern such as hexagonal array of wavelength-scale air holes running along the entire fiber length [2,3]. In such fibers, light guidance is provided either by modified total internal reflection [4] or by the photonic bandgap effect [5]. The unusual optical properties of these photonic crystal fibers include single-mode guiding at all optical wavelengths [4]. Zero group-velocity dispersion at wavelengths around 800 nm [3,6], and the possibility of designing fibers with an almost wavelength-independent dispersion[3,7].

Control radiative properties of materials by introducing a random refractive index variation, were theoretically proposed by Yablonovitch and John almost simultaneously in 1987. Yablonovitch suggested that photonic crystals could change the properties of the radiation field in such a way that there would be no electromagnetic modes available in the dielectric structure. It has been predicted and experimentally verified that the removal of dielectric materials in a PBG structure will generate a single mode in the gap, while addition of extramaterials will give rise to several modes. [8]

Arguably the most general numerical methods for electromagnetism are those that simulate the full time-dependent Maxwell equations, propagation the fields in both space and time, such time-domain methods can easily support strongly nonlinear or active (time-varying) media[9].

The most common technique for time-domain simulations is the finite-difference time-domain method, or FDTD. As the name implies, FDTD divides space and time into a grid (usually uniform) of discrete points and approximates the derivatives (Δ x and δ/δt) of the Maxwell equations by finite differences [9, 10]. One of the most studied and reliable methods are the plane wave expansion method. It was used in some of the earliest studies of photonic crystals [11-14] and is simple enough to be easily implemented.

Plane wave method represents unknown functions as a series expansion in complete basis set of smooth functions, truncating the series to have a finite number of terms.

Archetypically, a Fourier series is used, where the terms in the Fourier series are plane waves [9].

In this work, we calculate the cladding's photonic bandgap structure and photonic crystal states for the hollow core photonic crystal fibers. The cladding of these fibers can be considered as a 2D hexagonal array of air holes embedded in silica material. We consider propagation in the plane of periodicity.

Photonic Bandgap Structure:

Plane wave Expansion Method allows the computing of eigenfrequencies for a photonic crystal to any prescribed accuracy, commensurate with computing time [16], is based on the Fourier expansion of the internal field and the dielectric function [17]. The Fourier transform of electric and magnetic field is as follow [18].

$$-\left|k+G\right|^2 E_G + (\frac{w}{c})^2 \sum \varepsilon(G-G')E_{G'} = 0 \quad (1)$$

$$-(k+G).\sum_{G'}(G-G')\eta(G-G')H_{G'} + (\frac{w}{c})^2 H_G + (\frac{w}{c})^2 H_G = 0 \quad (2)$$

The cladding of HC-PCF is 2D triangular lattice of air holes embedded in a dielectric background; the dielectric function will be periodic only in the *x-y* plane (uniform in the *z* direction).

A triangular lattice and its reciprocal lattice are depicted in Fig. (1) [19]. The triangular lattice in Fig. (1) has b1 and b2 as its basis vectors, where and $b1 = a\hat{e}_x$ $b2 = (a/2)\hat{e}_x + (\sqrt{3}a/2)\hat{e}_y$

The corresponding reciprocal lattice vectors are $G1 = (2\pi/a)[\hat{e}_x - (1/\sqrt{3})\hat{e}_y]$ and $G2 = (4\pi/\sqrt{3}a)\hat{e}_y$ also depicted in the same figure. The first BZ is a hexagon; the point at the center of the zone is called the Γ point; two other important points are shown, the K point $(2\pi\sqrt{3}a)\hat{e}_y$ and the M point $(2\pi/\sqrt{3}a)[(1/\sqrt{3})\hat{e}_x + \hat{e}_y]$

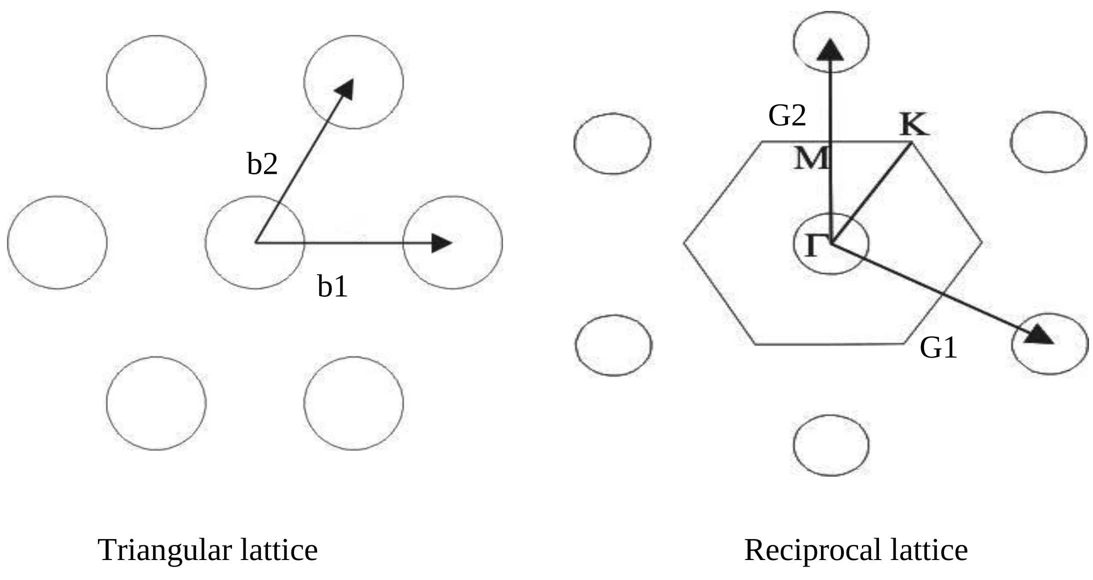

Fig. (1): A triangular lattice and Brilloun zone(BZ).

The band structure of HC19-1060 are shown in Fig. (2), Where n_a=1 and n_b=1.45, air filling fraction *f*= 90%, r/Λ=0.04474, n_a and n_b are the refractive index of air and silica respectively. r/Λ is the hole radius per lattice constant in rad/Sec. The width of TE- bandgap is equal to 0.036, and the upper and lower normalized

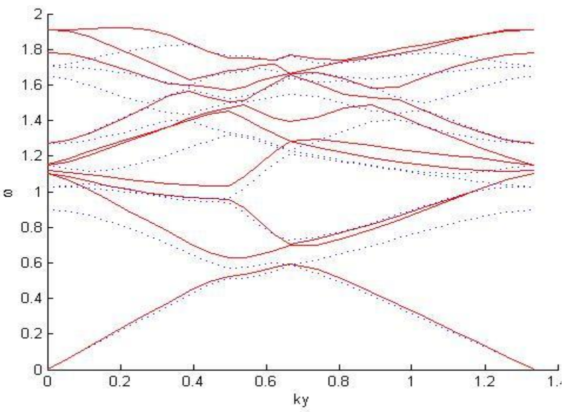

Fig. (2): Photonic band structure for HC19-1060 PC fiber.

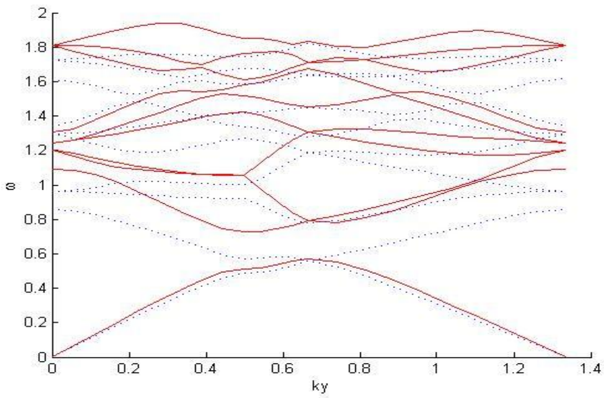

Fig. (3): Photonic band structure for HC7- 1060 PC fiber.

This type and other one of PC dispersion parameters are summarized in Table (1).The same structures are plotted for (HC7-1060) Photonic crystal fiber as shown in Fig.3 .

Table (1): Photonic Bandgap width for different types of HC-PC Fibers with n_a=1 and n_b=1.45.

HC –PC Fibers Types	r/Λ hole radius per lattice constant	Low normalized Frequency Band edge (rad/sec.)	High normalized frequency Band edge(rad/sec.)	Photonic Bandgap Width (rad/sec.)
HC19-1060	0.4474	0.5955	0.6315	0.036
HC7-1060	0.4069	0.5705	0.7259	0.1554

Photonic bandgap shift using methanol infiltrated photonic crystal fibers:

After filling these types with liquids have refractive index less than silica refractive index , then the bandgap become smaller than the case before filling, where filling HC19-1060 with methanol at 20 ^{0}C and refractive index n= 1.3247, decreases the width of the TE- bandgap from 0.036 in the case before filling to 0.012 in the case after filling. Photonic band structure after methanol filling HC19-1060 photonic crystal fiber is shown in Fig.(4).Increasing temperature of methanol infiltrated HC19-1060 PC fiber decreases the refractive index of methanol and increases the width of the TE-photonic bandgap of the photonic band structure, the results are shown in Table (2) and Figs. (5,6). There is slight decrease in high and low normalized frequency bandgap edge, the effect of heating appears on high normalized frequency band edge values more than low frequency band edge also this is presented in Fig.(5), There is rapid decay in photonic bandgap width with increasing methanol refractive index as shown in Fig.(6). Also from Table (2) the width of the gap increases with temperature and the maximum width is (0.0143) at temperature (70 ^{o}C) where relative refractive index is (1.3057).

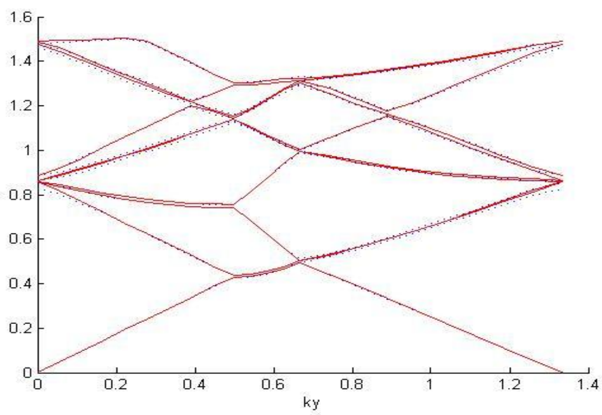

Fig. (4): Photonic band structure after methanol filling HC19-1060 PC fiber, refractive index is $n_{methanol}$ =1.3247, at 20 ^{o}C.

Table (2): Photonic Bandgap width of methanol infiltrated HC19-1060 PC fiber as a function to temperature.

Temperature(^{o}C)	methanol Refractive index ($n_{methanol}$)	Low normalized Frequency Band edge	High normalized frequency Band edge	Photonic Bandgap Width (rad/sec.)
20	1.3247	0.4266	0.4386	0.012
30	1.3209	0.4276	0.44	0.0124
40	1.3171	0.4285	0.4414	0.0129
50	1.3133	0.4295	0.4428	0.0133
60	1.3095	0.4304	0.4443	0.0139
70	1.3057	0.4314	0.4457	0.0143

Table (3): Photonic Bandgap width of methanol infiltrated HC7-1060 PC fiber as a function to temperature.

Temperature(^{o}C)	methanol Refractive index ($n_{methanol}$)	Low normalized Frequency Band edge	High normalized frequency Band edge	Photonic Bandgap Width (rad/sec.)
20	1.3247	0.4235	0.4436	0.0201
30	1.3209	0.4244	0.4453	0.0209
40	1.3171	0.4252	0.4469	0.0217
50	1.3133	0.426	0.4486	0.0226
60	1.3095	0.4269	0.4503	0.0234
70	1.3057	0.4277	0.452	0.0243

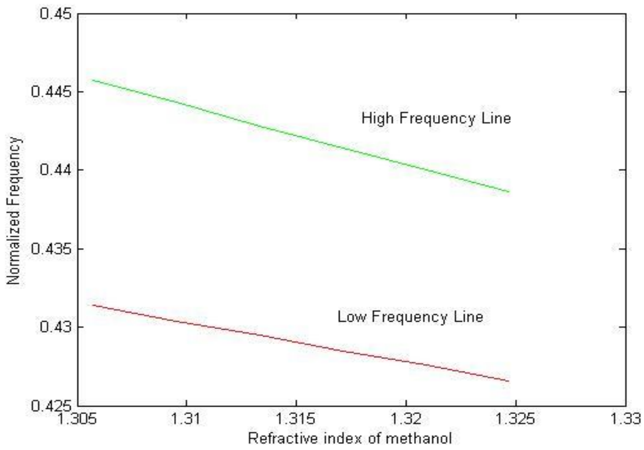

Fig.(5): HC19-1060 PC fiber bandgap edges as a function to refractive index of the infiltrated methanol with increasing temperature.

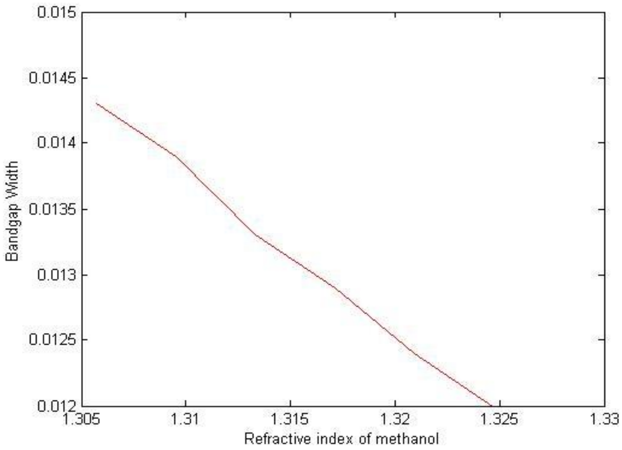

Fig. (6): Photonic bandgap width as a function to methanol refractive index with increasing temperature of methanol infiltrated HC19-1060 PC fiber.

Photonic bandgap shift using water infiltrated photonic crystal fibers:

The effect of infiltration of HC-PCFs with different liquids having refractive indices greater than air and less than silica to ensure bandgap mechanism on bandgap structure is considered. In this section we calculate the photonic bandgap shift and photonic crystal states by filling the set HC-PC fibers under study with distilled water. Fig. (7) illustrate photonic band for HC19-1060 PC fiber at 20 ^{o}C.The results of the photonic bandgap shift with increasing temperature of water infiltrated HC19-1060 PC and HC7-1060 PC fibers shown in Tables (4 and 5) respectively.

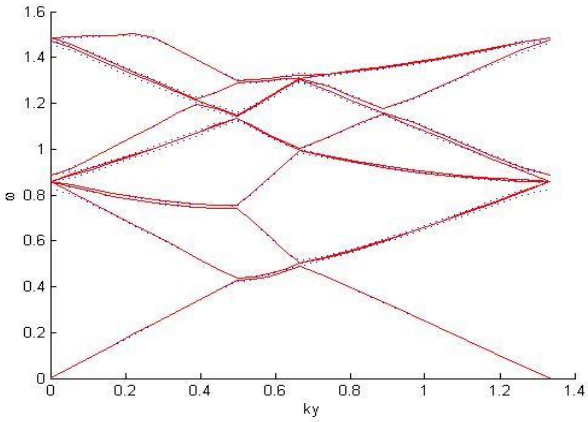

Fig. (7): Photonic band structure after water filling HC19-1060 PC fiber, refractive index is n_{water}=1.3277, at 20 ^{o}C.

Table (4): Photonic Bandgap width of water infiltrated HC19-1060 PC fiber as a function to temperature.

Temperature(^{o}C)	Water Refractive index (n_{water})	Low normalized Frequency Band edge	High normalized frequency Band edge	Photonic Bandgap Width (rad/sec.)
20	1.3277	0.4259	0.4375	0.0116
30	1.32736	0.426	0.4376	0.0116
40	1.32728	0.426	0.4376	0.0116
50	1.327208	0.426	0.4377	0.0117
60	1.32713	0.426	0.4377	0.0117
70	1.327054	0.426	0.4377	0.0117
80	1.326978	0.4261	0.4378	0.0117
90	1.32690	0.4261	0.4378	0.0117
100	1.32682	0.4261	0.4378	0.0117

Table (5): Photonic Bandgap width of water infiltrated HC7-1060 PC fiber as a function to temperature.

Temperature(^{o}C)	Water Refractive index (n_{water})	Low normalized Frequency Band edge	High normalized frequency Band edge	Photonic Bandgap Width (rad/sec.)
20	1.3277	0.4229	0.4423	0.0194
30	1.32736	0.4229	0.4424	0.0195
40	1.32728	0.423	0.4425	0.0195
50	1.327208	0.423	0.4426	0.0196
60	1.32713	0.423	0.4426	0.0196
70	1.327054	0.423	0.4426	0.0196
80	1.326978	0.423	0.4426	0.0196
90	1.32690	0.423	0.4426	0.0196
100	1.32682	0.4231	0.4427	0.0196

Photonic bandgap shift using n-hexane infiltrated photonic crystal fibers.

In this section we calculate the photonic bandgap shift by filling all HC-PC fibers under study with n-hexane. Also in this section we study the photonic band structure with different temperatures of n-hexane. Fig. (8) illustrate photonic band for HC19-1060 PC fiber at 20 ^{o}C.The results of the photonic bandgap shift with increasing temperature of n-hexane infiltrated HC19-1060 PC and HC17-1060 PC fibers are shown in Tables (6 and 7) respectively.

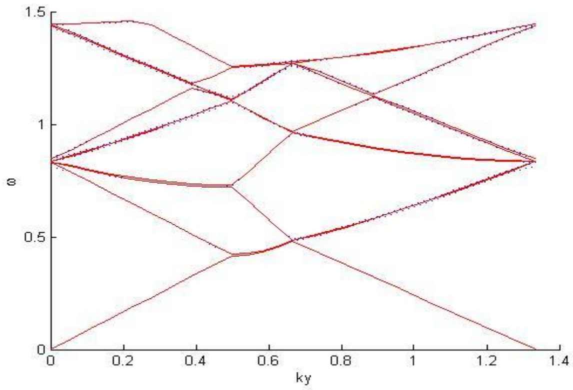

Fig. (8): Photonic band structure after hexane filling HC19-1060 PC fiber refractive index is n_{hexane}=1.3734, at 20 ^{o}C**.**

Table (6): Photonic Bandgap width of n-hexane infiltrated HC19-1060 PC fiber as a function to temperature.

Temperature(^{o}C)	n-hexane Refractive index (n_{hexane})	Low normalized Frequency Band edge	High normalized frequency Band edge	Photonic Bandgap Width (rad/sec.)
20	1.3734	0.415	0.4216	0.0066
30	1.3706	0.4157	0.4226	0.0069
40	1.3678	0.4163	0.4235	0.0072
50	1.365	0.417	0.4244	0.0074
60	1.3622	0.4177	0.4254	0.0077
70	1.3594	0.4183	0.4263	0.008

Table (7): Photonic Bandgap width of n-hexane infiltrated HC7-1060 PC fiber as a function to temperature**.**

Temperature(^{o}C)	n-hexane Refractive index (n_{hexane})	Low normalized Frequency Band edge	High normalized frequency Band edge	Photonic Bandgap Width (rad/sec.)
20	1.3734	0.4132	0.4241	0.0109
30	1.3706	0.4138	0.4252	0.0114
40	1.3678	0.4144	0.4262	0.0118
50	1.365	0.4149	0.4273	0.0124
60	1.3622	0.4155	0.4284	0.0129
70	1.3594	0.4161	0.4294	0.0133

Photonic bandgap shift using ethanol infiltrated photonic crystal fibers:

In this section we calculate the photonic bandgap shift by filling all HC-PC fibers under the study with ethanol. Also in this section we study the photonic band structure with different temperature of ethanol .Fig. (9) illustrate photonic band for HC19-1060 PC fiber at 20^{o}C.

The results of the photonic bandgap shift with increasing temperature of ethanol infiltrated HC19-1060 PC fiber shown in Table (8); increasing ethanol temperature from (20-70 ^oC) decreases the refractive index from (1.3568-1.3368). Increasing ethanol temperature from 20-70 ^oC increases photonic bandgap width from 0.0083 to 0.0105.

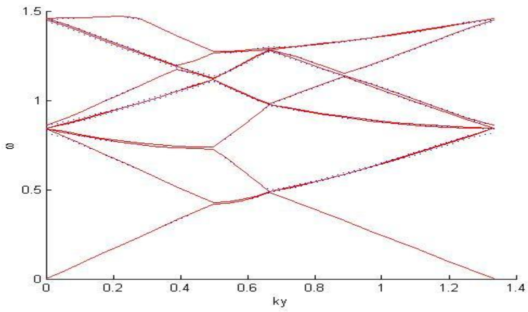

Fig. (9): Photonic band structure after ethanol filling HC19-1060 PC fiber, refractive index is $n_{ethanol}$ =1.3568, at 20 ^oC.

Table (8): Photonic Bandgap width of ethanol infiltrated HC19-1060 PC fiber as a function to temperature**.**

Temperature(^oC)	ethanol Refractive index ($n_{ethanol}$)	Low normalized Frequency Band edge	High normalized frequency Band edge	Photonic Bandgap Width (rad/sec.)
20	1.3568	0.4189	0.4272	0.0083
30	1.3528	0.4199	0.4286	0.0087
40	1.3488	0.4208	0.43	0.0092
50	1.3448	0.4218	0.4314	0.0096
60	1.3408	0.4227	0.4328	0.0101
70	1.3368	0.4237	0.4342	0.0105

The results of the photonic bandgap shift with increasing temperature of ethanol infiltrated HC17-1060 PC fiber shown in Table (9).

Table (9): Photonic Bandgap width of ethanol infiltrated HC7-1060 PC fiber as a function to temperature**.**

Temperature(^oC)	ethanol Refractive index ($n_{ethanol}$)	Low normalized Frequency Band edge	High normalized frequency Band edge	Photonic Bandgap Width (rad/sec.)
20	1.3568	0.4167	0.4305	0.0138
30	1.3528	0.4175	0.432	0.0145
40	1.3488	0.4183	0.4336	0.0153
50	1.3448	0.4192	0.4352	0.016
60	1.3408	0.42	0.4369	0.0169
70	1.3368	0.4209	0.4385	0.0176

Photonic bandgap shift using acetone infiltrated photonic crystal fibers:

In this section we calculate the photonic bandgap shift by filling all HC-PC fibers under the study with acetone. Also in this section we study the photonic band structure with different temperature of acetone.where Fig. (10) illustrate photonic band for HC19-1060 PC fiber at 20 ^oC.

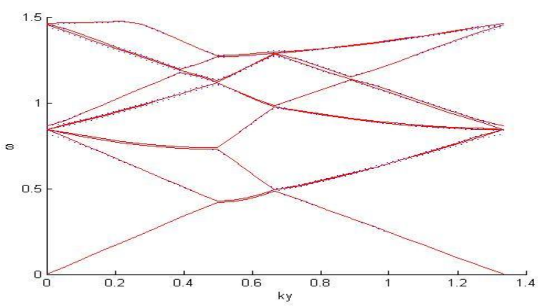

Fig. (10): Photonic band structure after acetone filling HC19-1060PC fiber, refractive index is $n_{acetone}$ =1.3540, at 20 ^oC.

The results of the photonic bandgap shift with increasing temperature of acetone infiltrated HC19-1060 PC fiber shown in Table (10); increasing acetone temperature from (20-70 ^{o}C) decreases the refractive index from (1.3540-1.328). Increasing acetone temperature from 20-70 ^{o}C increases photonic bandgap width from 0.009 to 0.0121.

Table (10): Photonic Bandgap width of acetone infiltrated HC19-1060 PC fiber as a function to temperature**.**

Temperature(^{o}C)	Acetone Refractive index ($n_{acetone}$)	Low normalized Frequency Band edge	High normalized frequency Band edge	Photonic Bandgap Width (rad/sec.)
20	1.3540	0.4194	0.4284	0.009
30	1.3488	0.4207	0.4302	0.0095
40	1.3436	0.4219	0.432	0.0101
50	1.3384	0.4231	0.4339	0.0108
60	1.3332	0.4244	0.4358	0.0114
70	1.328	0.4256	0.4377	0.0121

The results of the photonic bandgap shift with increasing temperature of acetone infiltrated HC17-1060 PC fiber shown in Table (11).

Table (11): Photonic Bandgap width of acetone infiltrated HC7-1060 PC fiber as a function to temperature**.**

Temperature(^{o}C)	Acetone Refractive index ($n_{acetone}$)	Low normalized Frequency Band edge	High normalized frequency Band edge	Photonic Bandgap Width (rad/sec.)
20	1.3540	0.4172	0.4316	0.0144
30	1.3488	0.4183	0.4336	0.0153
40	1.3436	0.4194	0.4357	0.0163
50	1.3384	0.4206	0.4379	0.0173
60	1.3332	0.4217	0.44	0.0183
70	1.328	0.4228	0.4422	0.0194

Refractive Index Scaling

Filling HC-PC fiber with liquids has refractive index less than silica refractive index n_{silica}=1.45, varied the low index medium. The result confirms a simple scaling law, where frequency shift of photonic bandgap demonstrated due to refractive index scaling [20]. The wave equation for the scalar field distribution in a photonic bandgap fiber is given by:

$$\nabla_T^2 \Psi(x,y) + (k^2 n_0^2 - \beta^2)\Psi(x,y) = 0 \quad (3)$$

Where k is the free-space wavenumber, n_0 is the transverse distribution of the refractive index of the structure, β is the propagation constant of the mode and ∇_T the transverse Laplacian operator. The scalar equation is strictly valid for very small index contrast; however it can still approximately describe propagation in a silica/air HC-PCF [21]. In the scalar case, for a photonic bandgap structure consisting of a material with high index n_1 and a material with low index n_2 with pitch Λ, it was found [21,22] that the photonic states scale so that the quantities:

$$v^2 = k^2\Lambda^2(n_1^2 - n_2^2) \quad (4)$$

$$w^2 = \Lambda^2(\beta^2 - k^2 n_2^2) \quad (5)$$

Remain invariant with any change of the parameters k, Λ, n_1 and n_2. Where v^2 is the frequency parameter and w^2 eigenvalue, n_1 and n_2 are the indices of the high and low index materials respectively.
These equations yield useful scaling laws that can describe the shift in frequency of the photonic states of the fiber when the index contrast of the latter is altered. When the low index material n_2 of the PCF is varied in Eqs.(4,5), while the high index n_1 remains unchanged, so that the initial index contrast $N_0=n_1/n_2$ becomes N, any bandgaps originally at a wavelength λ_0 will shift to a new wavelength λ given by [20,22].

$$\lambda = \lambda_0\left[\frac{1-N^{-2}}{1-N_0^{-2}}\right]^{1/2} \quad (6)$$

This scaling law is also particularly relevant to any application that requires filling the entire air region (core and cladding) of HC-PCF with gases or liquids [6]. The states of photonic crystal of HC-1060 are presented in Fig. (11).

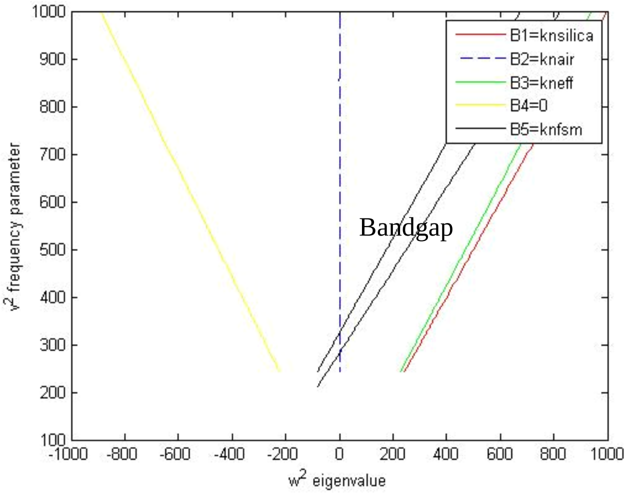

Fig. (11): The states of photonic crystal, on normalized axes V^2against eigenvalue W^2 for HC19-1060**.**

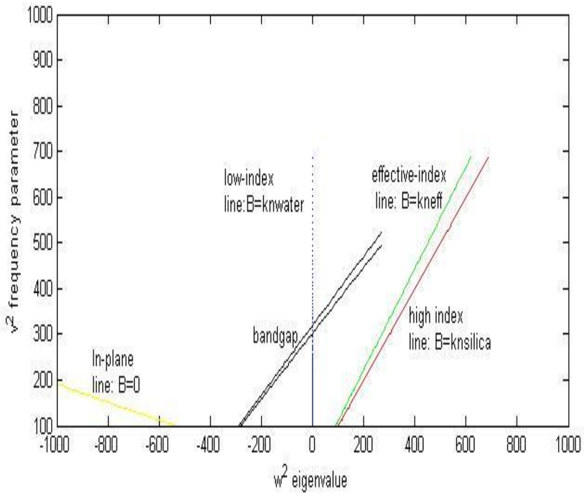

Fig. (12): The states of photonic crystal with water filling at 20 ^{0}C, on normalized axes V^2against eigenvalue W^2 for HC19-1060**.**

Photonic Bandgap finger in the states of HC-1060 photonic crystal fiber after filling with methanol will shifted from (1.0400-1.1100) µm the wavelength range between bandgap finger to (0.5700 – 0.5850) µm after filling with methanol depending on the scaling law, as shown in Fig.(12).

Conclusions

We have calculated the photonic band structure and photonic crystal states for the cladding of a hollow core crystal fibers. We show that the width of the photonic bandgap decreases with filling the air holes with liquids. The width of the photonic bandgap with infiltrated liquid at high temperature is larger than the bandgap of the same fiber with the same liquid but at room temperature. Maximum photonic bandgap width at (0.0243) has appeared with filling HC7-1060 PCF with methanol at 70 ^{0}C and refractive index (1.3057).

References

[1] Yan-feng Li, Ching-yue Wang and Ming-lie Hu "A fully vectorial effective index method for photonic crystal fibers: application to dispersion calculation", Opt. Commun. Vol. 238, Iss. 1-3, pp. 29-33, 2004 .

[2] J.C. Knight, T.A. Birks, P.St. Russell, and D.M.Atkin, "All-silica single-mode optical fiber with photonic crystal cladding" Optics Letters, Vol.21 Nol9,pp 15471549 October 1.1996.
[3] Martijn van Eijkelenborg, John Canning, Tom Ryan, and Katja Lyytikainen, "Bending-induced colouring in a photonic crystal fibre", Optics Express, Vol. 7, Issue 2, pp. 88-94 (2000)
[4] T. A. Birks, J. C. Knight, and P. St. Russell, "Endlessly single-mode photonic crystal fiber", Optics Letters, 22(13):961-963, 1997
[5] J.C. Knight, J. Broeng, T.A. Birks, and P.St. Russell, "Photonic Band Gap Guidance in Optical Fibers" Science 282, 1476 (1998).
[6] J. Ranka, R.S. Windeler, and A.J. Stentz, "Visible continuum generation in air-silica microstructure optical fibers with anomalous dispersion at 800 nm," Opt. Lett. 25, 25-27 (2000).
[7] J. Broeng, D. Mogilevstev, S.E. Barkou, and A. Bjarklev, “Photonic crystal fibers: A new class of optical waveguides,” Optical Fiber Technology , 5, 305–330, (1999).
[8] M. Johri, Y. A. Ahmed, and T. Bezboruah, “Photonic band gap materials: technology, applications and challenges,” Curr. Sci. 92, 1361–1365 (2007)
[9] J. D. Joannopoulos, S. G. Johnson, R. D. Meade, and J. N. Winn, Photonic Crystals: Molding the Flow of Light, second edition, Princeton Univ. Press (2008).
[10] Allen Taflove, Susan C. Hagness, "Computational Electrodynamics: The Finite-Difference Time-Domain Method", 3rd edition, Artech House (2005*).*
[11] M. Plihal and A. A. Maradudin, "Photonic band structure of 2D systems: the triangular lattice," Phys. Rev. B 44, 8565-8571 (1991).
[12] P. R. Villeneuve and M. Piche, "Photonic band gaps in two-dimensional square lattices: Square and circular rods", Phys. Rev. B 46, 4973-4975 (1992).
[13] R. D. Mead, K. D. Brommer, A. M. Rappe, and J. D. Joannopoulos, "Existence of a photonic band gap in 2-D," Appl. Phys. Lett. 61, 495–497(1992).
[14] K. M. Ho, C. T. Chan, and C. M. Soukoulis, “Existence of a Photonic Gap in Periodic Dielectric Structures”, Phys. Rev. Lett. 65, 3152 (1990).[15] Shruti, R. K. Sinha and R. Bhattacharya, "Anti-resonant reflecting Photonic Crystal Waveguide (ARROW): Modelling and Design", Optical and Quantum Electronics, Vol. 4, pp 181-187, (2009).
[16] Aaron Danner, Optical Device Research Group at the National University of Singapore, http://www.ece.nus.edu.sg/stfpage/eleadj/
[17] Kazuaki Sakoda, "Optical Properties of Photonic Crystals", Springer (2005).
[18] A. Lakhtakia, *Nanometer Structures: Theory, Modeling, and Simulation*, Handbook of Nanotechnology, Bellingham, WA: SPIE Press (2004)
[19] M. Marrone, V. F. Rodriguez-Esquerre and H. E. Hernandez-Figueroa, "Novel numerical method for the analysis of 2D photonic crystals: the cell method," Opt. Express 10, 1299-1304 (2002).
[20] G. Antonopoulos, F. Benabid, T. A. Birks, D. M. Bird, J. C. Knight, and P. St. J. Russell, "Experimental demonstration of the frequency shift of bandgaps in photonic crystal fibers due to refractive index scaling", Opt. Express,14,3000-3006 (2006).
[21]T. A. Birks, D. M. Bird, T. D. Hedley, J. M. Pottage, and P. St. J. Russell, "Scaling laws and vector effects in bandgap-guiding fibres," Opt. Express 12, 69-74 (2004).
[22] G. Antonopoulos, "Super-Enhanced Stimulated Raman Scattering And Particle Guidance In Hollow-Core Photonic Crystal Fibres", Ph. D. thesis, University of Bath, (2007).

مؤشر معامل الانكسار للميثانول المرتشح خلال ليف بلوري فوتوني ذي قلب فارغ

عبدالهادي الجنابي داليا حسين

معهد الليزر للدراسات العليا ، جامعة بغداد ، بغداد ، العراق

الخلاصة: تم في هذا البحث دراسة محاكاة لحساب مقدار الازاحة الترددية لليف بلوري فوتوني نتيجة تغير مؤشر معامل الانكسار من خلال ارشاح سوائل خلاله. تم ارشاح الميثانول ليملئ القلب والغطاء لليف الفوتوني البلوري نوع HC19-1060. ان ارشاح الميثانول يؤدي الى تغير المؤشر المعامل الفعال مع الغلاف.ان تأثير زيادة درجة الحرارة عل عرض فجوة النطاق وعلى خاصية النفاذية الضوئية قد تم حسابها .لقد وجد ان اعلى عرض للنطاق الفوتوني هو 0.0243 عند ارتشاح القلب والغطاء بالميثانول عند درجة حرارة 70مئوية يقابلها معامل انكسار 1.3057 .ان تركيب فجوة النطاق الفوتونية بالاتجاهين لبلورة فوتونية ذات بعدين وشبيكة ثلاثية مغروسة بالسيلكا تمت دراستها ايضا بأستخدام طريقة توسع الموجة المستوي لايجاد الشكل الاصبعي لفجوة النطاق الفوتوني في مرتسم البلورات الفوتونية.